Available online at www.sciencedirect.com
SCIENCE DIRECT®
Bioorganic & Medicinal Chemistry 12 (2004) 5799–5806
Bioorganic & Medicinal Chemistry

Preferential target is mitochondria in α-mangostin-induced apoptosis in human leukemia HL60 cells

Kenji Matsumoto,[a,*] Yukihiro Akao,[a] Hong Yi,[a] Kenji Ohguchi,[a] Tetsuro Ito,[b] Toshiyuki Tanaka,[b] Emi Kobayashi,[c] Munekazu Iinuma[c] and Yoshinori Nozawa[a]

[a]*Gifu International Institute of Biotechnology, 1-1 Naka-Fudogaoka, Kakamigahara, Gifu 504-0838, Japan*
[b]*Gifu Prefectural Institute of Health and Environmental Sciences, 1-1 Naka-Fudogaoka, Kakamigahara, Gifu 504-0838, Japan*
[c]*Gifu Pharmaceutical University, 5-6-1 Mitahora-higashi, Gifu 502-5858, Japan*

Received 7 July 2004; revised 26 August 2004; accepted 26 August 2004
Available online 16 September 2004

Abstract—Our previous study has shown that α-mangostin, a xanthone from the pericarps of mangosteen, induces caspase-3-dependent apoptosis in HL60 cells. In the current study, we investigated the mechanism of apoptosis induced by α-mangostin in HL60 cells. α-Mangostin-treated HL60 cells demonstrated caspase-9 and -3 activation but not -8, which leads us to assume that α-mangostin may mediate the mitochondrial pathway in the apoptosis. Parameters of mitochondrial dysfunction including swelling, loss of membrane potential ($\Delta\Psi m$), decrease in intracellular ATP, ROS accumulation, and cytochrome c/AIF release, were observed within 1 or 2 h after the treatment. On the other hand, α-mangostin-treatment did not affect expression of bcl-2 family proteins and activation of MAP kinases. These findings indicate that α-mangostin preferentially targets mitochondria in the early phase, resulting in indication of apoptosis in HL60 cells. Furthermore, we examined the structure–activity relationship between xanthone derivatives including α-mangostin and the potency of $\Delta\Psi m$-loss in HL60 cells. Interestingly, replacement of hydroxyl group by methoxy group remarkably decreased its potency. It was also shown that the cytotoxicity substantially correlated with $\Delta\Psi m$ decrease. These results indicate that α-mangostin and its analogs would be candidates for preventive and therapeutic application for cancer treatment.

1. Introduction

In recent years, many dietary factors and natural products have been evaluated as potential chemopreventive or therapeutics agents.[1] The pericarps of mangosteen, *Garcinia mangostana* Linn., have been used as a traditional medicine for treatment of skin infection and wounds in Southeast Asia for many years, and xanthones from the pericarps have been attracted as useful sources of chemopreventive or therapeutic agents, because of their biological activities containing antibacterial activity,[2] anti-inflammatory,[3] anticancer,[4,5] and inhibition of prostaglandin E2 synthesis.[6] Our previous study has reported potent cytotoxic activity of six xanthones from mangosteen against human leukemia HL60 cells.[5] Among them, α-mangostin showed the strongest activity and induced apoptosis in human leukemia cell lines HL60, K562, NB4, and U937 at 10 μM, at which concentration no cytotoxic effect was observed in concanavalin A-stimulated human peripheral blood lymphocytes.

It is well known that mitochondria play a crucial role in apoptosis.[7] One of the major and important parameter of mitochondrial dysfunction is the loss of mitochondrial membrane potential ($\Delta\Psi m$).[8] Loss of $\Delta\Psi m$ results in compromising ATP production and can trigger the release of apoptogenic factors including cytochrome c, apoptosis inducing factor (AIF), Smac/Diablo, and EndoG from mitochondria into cytosol, leading to cell death.[9] Recently, the design of mitochondrion-targeted therapeutic strategies for cancer has been attempted.[10–12] For example, Muscarella et al. have reported that pretreatment of PK11195, a ligand to peripheral benzodiazepin receptor on mitochondria, can sensitize drug-resistant EW36 cells to apoptosis.[13]

In the present study, we have extended our earlier study[5] to examine the mechanism of cell death induced by α-mangostin treatment in human leukemia cell line HL60. Furthermore, the structure–activity relationship

Keywords: α-mangostin; Xanthone; Mitochondrial dysfunction.
* Corresponding author. Tel.: +81 583 71 4646; fax: +81 583 71 4412; e-mail: kmatsumo@giib.or.jp

0968-0896/$ - see front matter © 2004 Elsevier Ltd. All rights reserved.
doi:10.1016/j.bmc.2004.08.034

was investigated in xanthone derivatives including α-mangostin, based on the potency of $\Delta\Psi m$ loss in HL60 cells.

2. Materials and method

2.1. Materials

Xanthones used in this study were purified as described in our previous study.[14] Compound 4 was obtained from partial methylation of compound 3. Their purity with over 98% was confirmed by high-performance liquid chromatography analysis (data not shown). Caspases Colorimetric Protease Assay Kit (acetyl-VDVAD-*p*-nitroanilide (Ac-VDVAD-*p*NA) for caspase-2, Ac-DEVD-*p*NA for caspase-3, Ac-IETD-*p*NA for caspase-8, Ac-LEHD-*p*NA for caspase-9) were purchased from MBL (Nagoya, Aichi, Japan). Mito Tracker Orange CM-H_2TMRos, and CM-H2DCFDA were obtained from Molecular Probes (Eugene, OR, USA). zVAD.fmk (*N*-Benzyloxycarbonyl-valine-alanine-aspartic acid(O–Me) fluoromethyl ketone), zFA.fmk (*N*-benzyloxycarbonyl-phenylalanine-alanine fluoromethyl ketone), Resveratrol and Taxol (Paclitaxel) were purchased from Sigma (St. Louis, MO, USA).

2.2. Cell culture and treatments

Human M2-type leukemia cell line HL60 was provided by RIKEN Cell Bank (Tsukuba, Ibaraki, Japan). Cells were cultured in RPMI-1640 medium containing 10% heat-inactivated fetal bovine serum. Xanthones dissolved in DMSO was added to the cell cultures with final DMSO concentration of 0.05% v/v, which had no significant effect on the growth and differentiation of HL60 cells (data not shown). Viable cell number was measured by trypan-blue dye exclusion test using Thoma type cell count chamber.

2.3. Hoechst 33342 staining

For morphological examination of apoptotic changes, cells were stained with Hoechst 33342 (Calbiochem, San Diego, CA, USA). Hoechst 33342 was added to cultured medium at a concentration of 5 μg/mL. After incubation for 30 min, cells were collected and washed with phosphate-buffered saline (PBS) and then observed under a fluorescence microscope, Olympus BX-51 (Olympus, Tokyo, Japan).

2.4. DNA extraction and agarose gel electrophoresis

The cells treated or untreated with α-mangostin (10 μM) were collected and washed with PBS. Cells were incubated at 37 °C overnight with 100 mM Tris–HCl (pH 7.4), 5 mM EDTA, 200 mM NaCl, 0.2% SDS, and 200 μg/mL proteinase K (Takara, Otsu, Shiga, Japan) and then extracted with phenol/chloroform. DNA was precipitated with ethanol and then treated with 0.1 mg/mL RNaseA (Sigma). DNA (2 μg) was analyzed by electrophoresis on 2% agarose gel.

2.5. Electron microscopy

The cells treated or untreated with α-mangostin (10 μM) were harvested and rinsed with PBS. Cells were fixed for 30 min in 4% paraformaldehyde and 1% glutaraldehyde in 0.1 M phosphate buffer (pH 7.4) (PB), rinsed in PB, and postfixed in 1% osmium tetraoxide for 30 min. After washing in PB, cells were progressively dehydrated in a 10% graded series of 50–100% ethanol and then cleared in QY-1 (Nissin EM, Tokyo Japan). Cells were embedded in Epon 812 resin (TAAB Laboratories Equipment, Reading, UK), and thin sections (70 nm thickness) were stained with uranyl acetate and lead citrate, and then examined by transmission electron microscopy, JEM-120 (JEOL, Tokyo, Japan), operating at 80 kV.

2.6. Measurement of mitochondrial membrane potential ($\Delta\Psi m$) by fluorescence-augmented cell sorter (FACS)

$\Delta\Psi m$ was measured by use of a Mito Tracker Orange CM-H_2TMRos, which accumulates selectively in active mitochondria and becomes to be fluorescent when oxidized. The cells treated or untreated with α-mangostin and other xanthone derivatives were washed in RPMI-1640 medium, followed by incubation with Mito Tracker fluorescent probes (100 nM) for 20 min at 37 °C. After washing with PBS, the cells were resuspended in PBS. Flow cytometry was performed over 20,000 events by three-color flow cytometry with a modified FACS Calibor cytometer and CellQuest software (Becton Dickinson, San Joes, CA, USA). The laser emission at 534–606 nm was used for detection of orange fluorescence, with excitation at 488 nm.

2.7. Antibodies and western blotting

We used antibodies against: mouse monoclonal anti-cytochrome *c* (Upstate, Charlottesville, VA, USA), rabbit polyclonal anti-AIF (ΨPro Sci, Poway, CA, USA), mouse monoclonal anti-Bcl2 and -Bcl-XL, and rabbit polyclonal anti-Bax and anti-Caspase-3 (Santa Cruz Biotechnology, Santa Cruz, CA, USA), rabbit polyclonal anti-Bid, anti-phospho-p38, anti-phospho-ERK, and anti-phospho-JNK (Cell Signaling, Beverly, MA, USA), mouse monoclonal anti-caspase-8 (MBL), mouse monoclonal anti-Ccaspase-9 (NOVUS Biologica, Littleton, CO, USA), and mouse monoclonal anti-β-actin (Sigma). The cells treated or untreated with α-mangostin were harvested and rinsed with ice-cold PBS. For preparation of cell lysate, the cell pellet was resuspended in lysis buffer A containing 10 mM Tris–HCl pH 7.4, 1% NP-40, 0.1% deoxycholic acid, 0.1% SDS, 150 mM NaCl, 1 mM EDTA, 1% Phosphatase Inhibitor Cocktail I and II (Sigma), and 1% Protease Inhibitor Cocktail (Sigma) and stood for 30 min on ice. After centrifugation at 14,000 rpm for 20 min at 4 °C, the supernatant was collected as the cell lysate. On the other hand, the cytosolic fraction was prepared as follows. The cells were resuspended in lysis buffer B containing 20 mM Hepes–KOH (pH 7.5), 10 mM $MgCl_2$, 1 mM EDTA, 1 mM EGTA, 1 mM dithiothreitol, 250 mM sucrose, and 1% Protease Inhibitor Cocktail and incubated on ice for 30 min. Plasma membrane fragments and nuclei

were removed by centrifugation at 10,000 rpm for 20 min at 4 °C, and the resultant supernatant was used as the cytosolic fraction. Protein content was measured with a DC Protein assay kit (BIORAD, Hercules, CA, USA). Five micrograms of protein of each sample was analyzed as previously described in our previous study.[5] For detection of β-actin used as an internal control, membranes were reprobed by using a Restore Western Blot Stripping Buffer (PIERCE, Rockford, IL, USA).

2.8. Quantification of ATP levels

The ATP concentration in the cells treated or untreated with α-mangostin (10 μM) was measured with ATP HS-II assay kit (Roche, Mannheim, Germany) in a luminofluorometer (TD-20/20, Promega, Madison, WI, USA) according to the manufacture instruction.

2.9. Assessment of intracellular ROS accumulations by FACS

The cells treated or untreated with α-mangostin (10 μM) were washed in RPMI-1640 medium, followed by incubation with CM-H2DCFDA probes (100 nM each) in Ringer-Locke solution for 10 min at 37 °C. After washing with PBS, the cells were resuspended in PBS. Flow cytometry was performed over 20,000 events by three-color flow cytometry with a modified FACSCalibor cytometer and CellQuest software. The laser emission at 515 nm was used for detection of green fluorescence with excitation at 488 nm.

2.10. Caspase activity assay

Activities of caspases-2, -3, -8, and -9 were measured by the colorimetric assay with Colorimetric Protease Assay Kit. Briefly, the cells treated or untreated with α-mangostin (10 μM) were washed twice in ice-cold PBS and cell lysates were obtained according to manufacturer instruction. The cell lysates containing 100 μg of protein were incubated with *p*NA-conjugated substrates and the release of *p*NA was measured at 405 nm using a microplate reader NJ-2300 (NUNC, Rockilde, Denmark).

2.11. Statistics

In statistical analysis, we performed one-way ANOVA or student *t*-test using a StatView software (SAS Institute Inc., Cary, NC).

3. Results

3.1. Apoptosis induced by α-mangostin in HL60 cells

α-Mangostin (Fig. 1) induces typical apoptosis accompanying DNA ladder formation (Fig. 2A) and nuclear condensation and fragmentation (Fig. 2B) in HL60 cells within 12 h. To examine mechanisms of α-mangostin-induced apoptosis in HL60 cells, we have measured the caspase activities following the α-mangostin treatment (Fig. 3). α-Mangostin induced activation of caspase-9 after 2 h of incubation, which was followed by caspase-3 activation. There was a small but significant increase in caspase-2 activity at 12 h of incubation. Caspase-8 activity remained unchanged. Except for caspase-2, other caspases activation was confirmed by Western blot analysis (data not shown). Thus, α-mangostin-induced apoptosis was thought to be mediated by the caspase-9/caspase-3 pathway. From the temporal profile of caspase-2 activation, it may contribute to amplification of the apoptotic pathway.

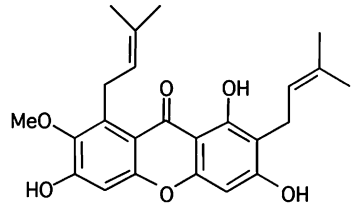

α-Mangostin

Figure 1. Chemical structures of α-mangostin.

3.2. Mitochondrial dysfunctions in α-mangostin-treated cells

The caspase-9/caspase-3 pathway is the underlying mitochondrial pathway of apoptosis. To examine the effect of α-mangostin on mitochondria, we investigated various parameters of mitochondrial dysfunction after 10 μM of α-mangostin treatment. Electron microscopic observations indicated mitochondrial swelling at 1 h after incubation with α-mangostin (Fig. 4A). The release of cytochrome *c* and AIF into cytoplasm was detected at 1 and 3 h, respectively (Fig. 4B). Decreases in $\Delta\Psi m$ (Fig. 4C), ROS accumulation (Fig. 4D), and decrease in intracellular ATP level (Fig. 4E) were also observed at 1 h after the treatment. These results indicated mitochondrial dysfunctions induced by α-mangostin in HL60 cells. It was also shown that these mitochondrial events preceded the caspase activation cascade.

3.3. zVAD.fmk blocks apoptosis but not decrease in $\Delta\Psi m$ induced by α-mangostin

In view of our results demonstrating caspase-9 and -3 activation in α-mangostin-induced apoptosis, we tested the ability of general caspase inhibitor, zVAD.fmk, to protect apoptosis induced by α-mangostin in HL60 cells. We pre-incubated cells with 100 μM of zVAD.fmk for 1 h and then stimulated cells with 10 μM of α-mangostin. As a negative control, zFA.fmk was used. As shown in Figure 5A, zVAD.fmk pretreatment significantly protected cell death induced by α-mangostin. Hoechst 33342 staining showed significant decrease in the proportion of apoptotic cells by the pretreatment with zVAD.fmk (Fig. 5B). These results suggest that caspases play crucial role in the α-mangostin-induced apoptosis in HL60 cells. Next, to examine whether the decrease in $\Delta\Psi m$ induced by α-mangostin was dependent on caspases activation, we measured $\Delta\Psi m$ by FACS using Mito Tracker Orange. Figure 5C showed that $\Delta\Psi m$ changes by α-mangostin treatment was not influenced by zVAD.fmk, indicating that the decrease in $\Delta\Psi m$ was not an event secondary to caspases activation.

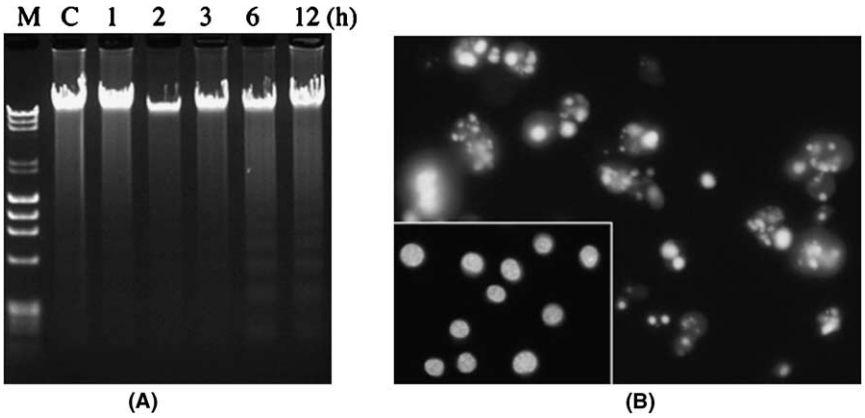

Figure 2. α-Mangostin-induced apoptosis in HL60 cells. Cells were treated with 10 μM α-mangostin and harvested at indicated incubation times. (A) Nucleosomal DNA fragmentation (M, DNA size marker; C, untreated control). (B) Morphological examination by Hoechst 33342 staining (magnification, ×400) after 12 h treatment. Inset indicates control cells (×200).

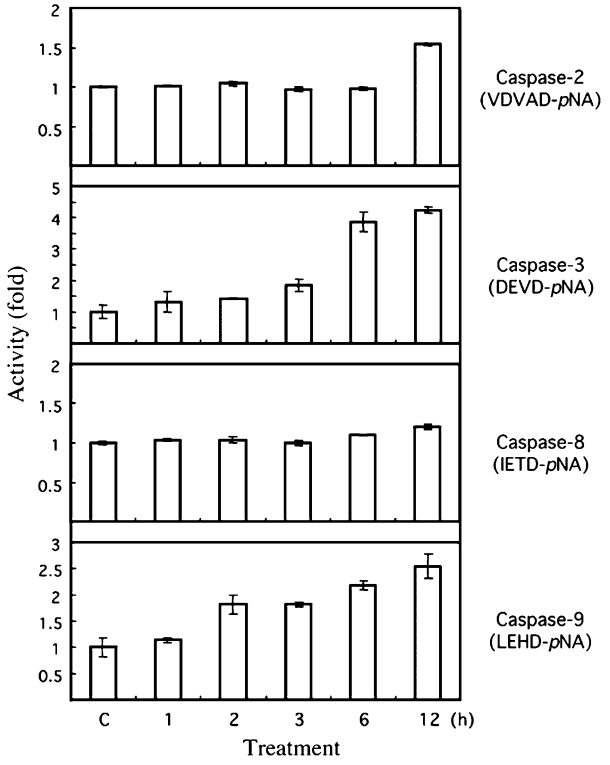

Figure 3. Activities of various caspases in α-mangostin (10 μM)-treated HL60 cells. Cells were collected at indicated time intervals after 10 μM α-mangostin treatment and subjected to the caspase activity assay using Caspase Colorimetric Protease Assay Kits. Data are expressed as means ± SD of three different experiments.

3.4. Expression of bcl-2 family proteins and MAPK signaling in α-mangostin-induced apoptosis

Bcl-2 family proteins have been known to regulate $\Delta\Psi m$ and the apoptogenic factor release from mitochondria.[15] We have then examined involvement of Bcl-2 family in α-mangostin-induced apoptosis in HL60 cells. Figure 6A showed no apparent changes in the expression levels of anti-apoptotic Bcl-2 and Bcl-xL and pro-apoptotic Bax. In the case of Bid, its expression apparently increased after the treatment, however, the cleaved active form (tBid) was not produced. These results indicate that these members of bcl-2 family are not involved in the α-mangostin-induced apoptosis. On the other hand, mitogen-activated protein kinases (MAPKs) have also been known to control a variety of physiological processes including cell proliferation and cell death, and there are three well-characterized subfamilies, ERK (-1 and -2), JNK (-1 and -2), and p38 MAPK.[16] It has been reported that some dietary phytochemicals induce apoptosis thorough MAPKs activation.[1] We examined MAPKs activation in α-mangostin-treated HL60 cells using anti-phospho-MAPKs antibodies. Activation of any MAPKs in α-mangostin-treated cells was not observed until 6 h when DNA ladder formation and caspase-3 activation occurred (Fig. 6B), indicating that MAPKs would not play a crucial role in α-mangostin-induced apoptosis.

3.5. Structure–activity relationship of xanthone derivatives in mitochondrial dysfunction

Loss of $\Delta\Psi m$ is a crucial dysfunction of mitochondria, because loss of $\Delta\Psi m$ induces release of apoptogenic factors into cytoplasm and decrease of ATP generation, leading to cell death.[7,9] In the present study, we have demonstrated that the preferential target of α-mangostin is mitochondria and induces their dysfunctions. To gain some insight into the structure–activity of the xanthones, we have examined the effects of other three xanthones (compound 1, 3, 4) similar to α-mangostin (compound 2) (Fig. 7A) on the mitochondrial dysfunction by measuring $\Delta\Psi m$ in HL60 cells (Fig. 7B). Interestingly, the ability to lower the $\Delta\Psi m$ was observed to be related with the number of hydroxy group (compound 1 > 2 > 3 > 4), and its replacement with methoxy group remarkably reduced the potency to decrease $\Delta\Psi m$.

3.6. Cytotoxic effect of α-mangostin and other xanthone derivatives

The collapse of $\Delta\Psi m$ was considered to be an irreversible step in the death cascade.[17] As the level of $\Delta\Psi m$ decline and cytotoxicity are thought to be closely related,

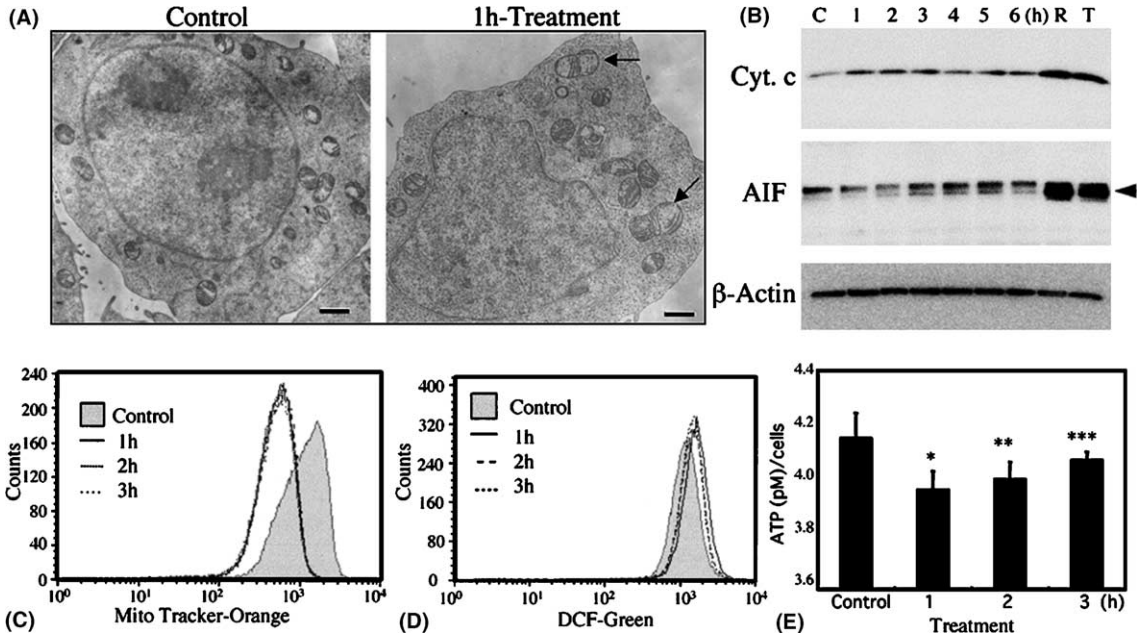

Figure 4. Mitochondrial dysfunctions induced by α-mangostin (10 μM) in HL60 cells. (A) Electron microscopic observations of α-mangostin (10 μM)-treated or untreated control cells for 1 h. Swollen mitochondria were shown (arrow). Bar indicates 1 μm. (B) Release of cytochrome *c* (Cyt. C) and apoptosis-inducing factor (AIF) into cytosol was detected by Western blot analysis. As positive controls, cells treated with 20 μM of resveratrol (R) and 0.1 μM of Taxol (T) for 24 h were used. β-Actin was used as an internal control. (C) Measurement of mitochondrial membrane potential ($\Delta\Psi m$) using Mito Tracker Orange by FACS at 1, 2, and 3 h after α-mangostin (10 μM) treatment. (D) Intracellular ROS accumulation measured by FACS using CM-H2DCFDA probe after the same treatment with α-mangostin. (E) Intracellular ATP content. Data are expressed as means ± SD of four different experiments. (*: $P < 0.001$, **: $P < 0.005$, ***: $P < 0.05$; Fisher's PLSD).

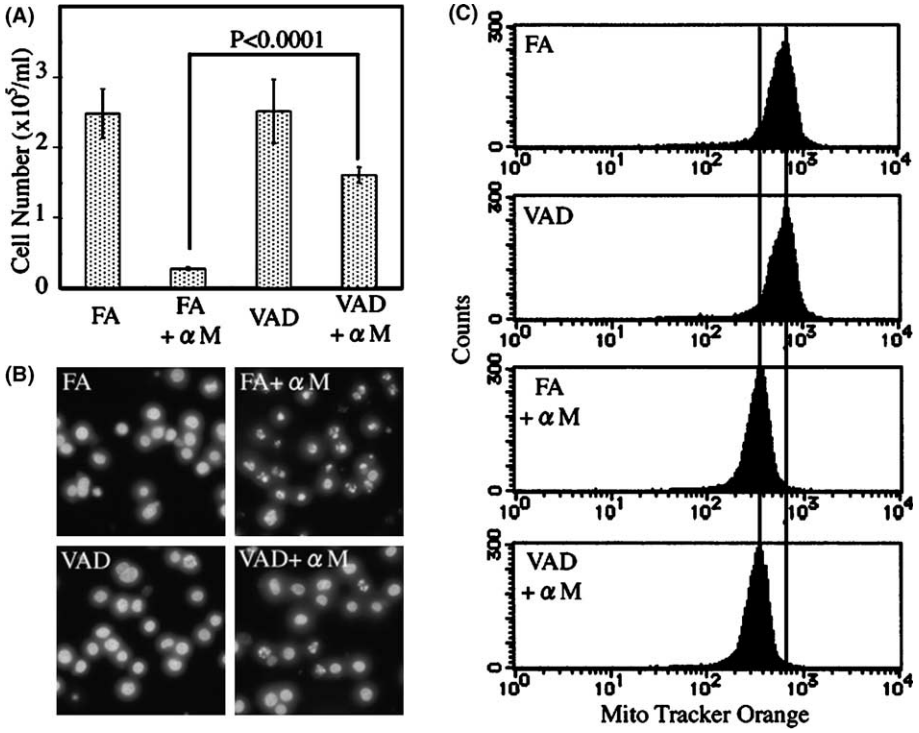

Figure 5. Effect of zVAD.fmk on α-mangostin-induced apoptosis. Cells were incubated in the presence of 100 μM zVAD.fmk (VAD) or zFA.fmk (FA) for 1 h prior to the addition of 10 μM α-mangostin (αM). (A) Viable cell number was measured by trypan-blue dye exclusion test at 24 h after the α-mangostin-treatment. Starting cell number is 2×10^5 cells/mL. Data are expressed as means ± SD of four different experiments. (*P* value was evaluated by Student *t*-test). (B) Morphological examination by Hoechst 33342 staining at 24 h after the α-mangostin-treatment (magnification, ×400). (C) Measurement of mitochondrial membrane potential ($\Delta\Psi m$) using Mito Tracker Orange by FACS at 1 h after the α-mangostin-treatment.

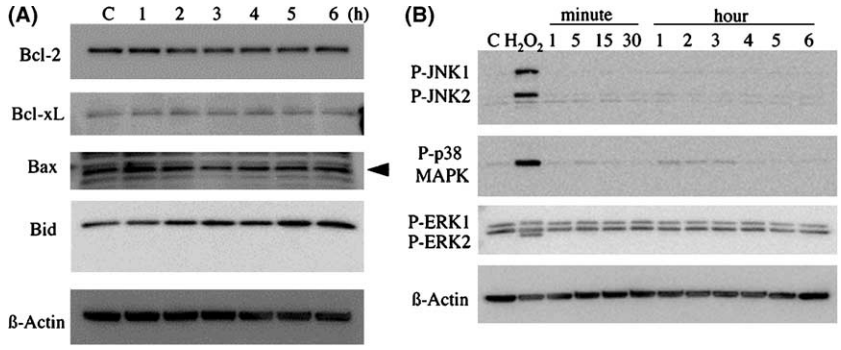

Figure 6. Western blot analysis of Bcl-2 family proteins (A) and phosphorylation MAPKs (B) in α-mangostin (10 μM)-treated HL60 cells. Cells were collected after the α-mangostin-treatment for up to 6 h. Cells treated with 0.5 mM H_2O_2 for 2 h were used as positive control for phospho-JNK1, JNK2 and p38 MAPK. β-Actin was used as an internal control.

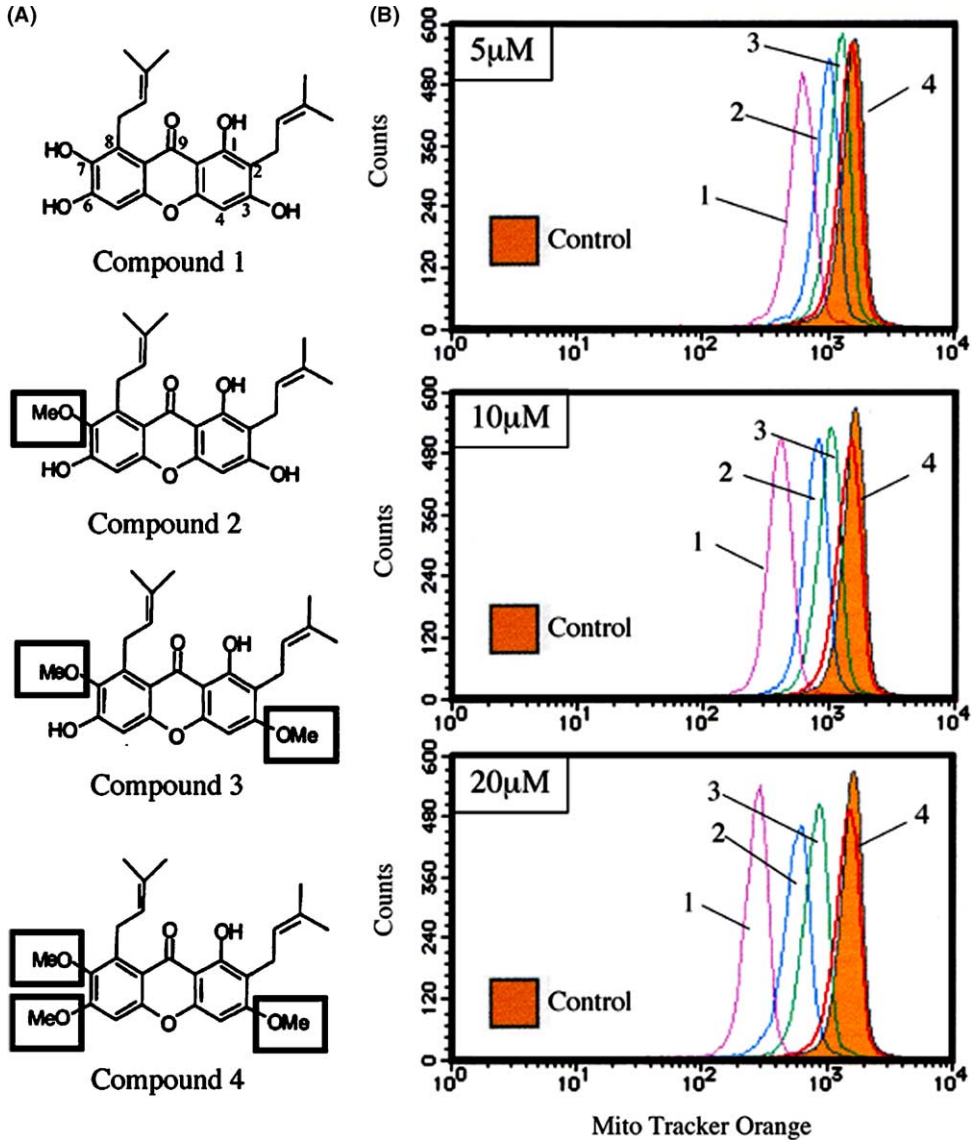

Figure 7. Chemical structures of various xanthones (A) and their effects on $\Delta\Psi m$ (B). $\Delta\Psi m$ was measured by FACS using Mito Tracker Orange at 1 h after the treatment of HL60 cells with xanthones at 5, 10, and 20 μM.

we have examined the cytotoxicity by α-mangostin and other xanthone derivatives against HL60 cells (Fig. 8). The cytotoxicity of xanthones was correlated with the level of $\Delta\Psi m$ reduction, but α-mangostin (compound

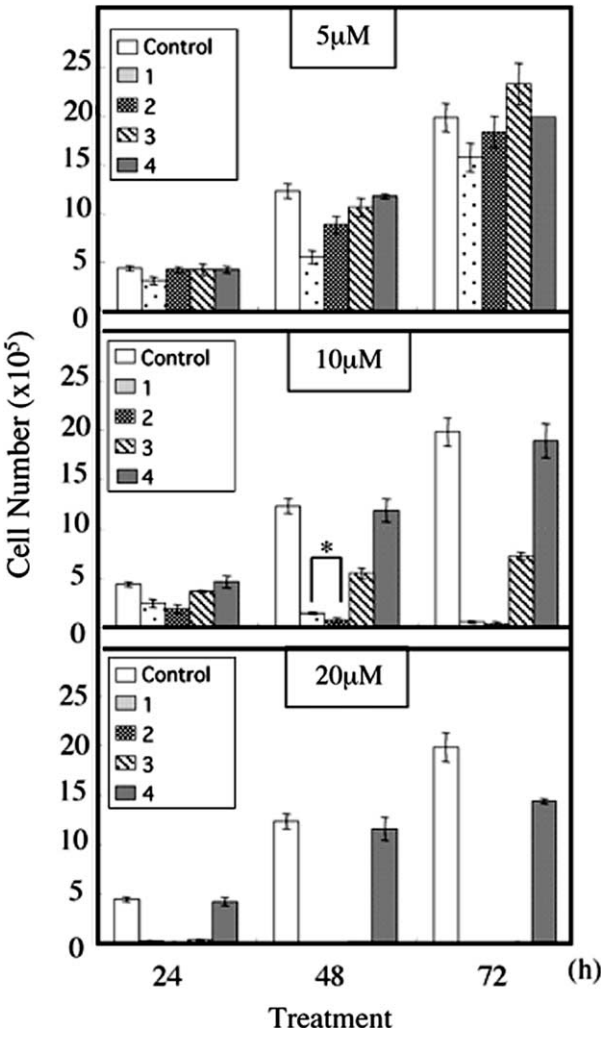

Figure 8. Dose-dependent cytotoxicity by α-mangostin and xanthones at 5, 10, and 20 μM. Compound 1–4 was same as indicated in Figure 7. Starting cell number is 2×10^5 cells/mL. Data are expressed as means ± SD of four different experiments. (*: $P < 0.005$; Student t-test).

2) exhibited stronger cytotoxicity than compound 1 at more than 10 μM at 48 h ($P < 0.005$).

4. Discussion

A number of papers describing tumor preventive and therapeutic activities of dietary phytochemicals have been reported during the last few years.[1] Although the putative cellular targets and the mechanisms of some compounds extracted from plants have been identified, their precise molecular mechanisms remain unclear. α-Mangostin has been demonstrated to induce apoptosis in cultured cell lines, such as human leukemia HL60, K562, NB4, and U937, and rat phenochromocytoma PC12.[5,18] However, the cellular target site or molecules has not yet been clarified.

Bcl-2 family proteins and MAPKs play important roles when apoptotic stimuli exert their effects on mitochondria.[7,15,19] On the other hand, caspase-8 and caspase-2 act upstream of the mitochondrial apoptotic pathway, such as death receptor stimulation and stress-induced apoptosis.[20,21] In the present study, we demonstrated that α-mangostin induced apoptosis in HL60 cells, which was mediated by mitochondrial dysfunctions in its early phase. There was no indication of activation of caspase-8 and MAPKs, and involvement of Bcl-2 family proteins in α-mangostin-induced cell death. In addition, although a general caspase inhibitor, zVAD.fmk significantly protected α-mangostin-induced apoptosis, decrease in $\Delta\Psi m$ induced by α-mangostin was not restored by zVAD.fmk. These data suggest that α-mangostin may directly act on mitochondria and induces apoptosis.

We have shown the cytochrome *c* release into cytoplasm and small but significant activation of initiator caspase-9, followed by caspase-3 activation within 3 h in α-mangostin treated HL60 cells. A pro-apoptotic factor, AIF release from mitochondria into cytoplasm and activation of caspase-2 acting upstream mitochondria were also observed, suggesting their amplifying roles in the mitochondrial apoptotic pathway, cytochrome c/caspase-9/caspase-3. Sato et al. reported α-mangostin-induced apoptosis via the mitochondrial associated with inhibition of Ca^{2+} ATPase pathway in rat pheochromocytoma PC12 cells.[18] Similar observations such as cytochrome *c* release, loss of $\Delta\Psi m$, activation of caspase-3 but not caspase-8, were also obtained in our system with HL60 cells. Although they demonstrated marked JNK activation, we were unable to detect it. This discrepancy was likely to be due to difference of cell type.

Since structures of α-mangostin and xanthone derivatives resemble the mitochondrial specific fluorescent dyes, dihydrorhodamine 123 and Mito Tracker Orange CM-H2TMRos, it is reasonable to consider that the xanthones may interact with or act on mitochondria. In fact, Wu et al. have reported that gaudichaudione A, a cytotoxic xanthone, induced mitochondrial destabilization.[22] Our present study demonstrated that α-mangostin and also other xanthones rapidly induce loss of $\Delta\Psi m$. The results shown here imply that the preferential target of xanthones is mitochondria.

Mitochondria play a pivotal role in induction of apoptosis and are thought to be a novel target of anti-cancer chemotherapy.[10–13] Actually, strategies for the development of anti-cancer agents acting on mitochondria are gathering attractive attention. Our present study provides a useful clue to consider α-mangostin and other xanthones as a candidate for developing new anti-cancer drugs. However, we need further extended experiments to define the structure–activity relationships of the xanthones tested here, which are under current progress in our laboratory.

Supplementary data

Supplementary data associated with this article can be found, in the online version, at doi:10.1016/j.bmc.2004.08.034.

References and notes

1. Surh, Y. J. *Nat. Rev. Cancer* **2003**, *3*, 768.
2. Iinuma, M.; Tosa, H.; Tanaka, T.; Asai, F.; Kobayashi, Y.; Shimano, R.; Miyauchi, K. *J. Pharm. Pharmacol.* **1996**, *48*, 861.
3. Shankaranarayan, D.; Gopalakrishnan, C.; Kameswaran, L. *Arch. Int. Pharmacodyn. Ther.* **1979**, *239*, 257.
4. Ho, C. K.; Huang, Y. L.; Chen, C. C. *Planta Med.* **2002**, *68*, 975.
5. Matsumoto, K.; Akao, Y.; Kobayashi, E.; Ohguchi, K.; Ito, T.; Tanaka, T.; Iinuma, M.; Nozawa, Y. *J. Nat. Prod.* **2003**, *66*, 1124.
6. Nakatani, K.; Nakahata, N.; Arakawa, T.; Yasuda, H.; Ohizumi, Y. *Biochem. Pharmacol.* **2002**, *63*, 73.
7. Wang, X. *Genes Dev.* **2001**, *15*, 2922.
8. Kroemer, G. *Biochem. Biophys. Res. Commun.* **2003**, *304*, 433.
9. Ly, J. D.; Grubb, D. R.; Lawen, A. *Apoptosis* **2003**, *8*, 115.
10. Decaudin, D.; Marzo, I.; Brenner, C.; Kroemer, G. *Int. J. Oncol.* **1998**, *12*, 141.
11. Debatin, K. M.; Poncet, D.; Kroemer, G. *Oncogene* **2002**, *21*, 8786.
12. Galiegue, S.; Tinel, N.; Casellas, P. *Curr. Med. Chem.* **2003**, *10*, 1563.
13. Muscarella, D. E.; O'Brien, K. A.; Lemley, A. T.; Bloom, S. E. *Toxicol. Sci.* **2003**, *74*, 66.
14. Asai, F.; Tosa, H.; Tanaka, T.; Iinuma, M. *Phytochemistry* **1995**, *39*, 943.
15. Tsujimoto, Y. *J. Cell Physiol.* **2003**, *195*, 158.
16. Johnson, G. L.; Lapadat, R. *Science* **2002**, *298*, 1911.
17. Zamzami, N.; Marchetti, P.; Castedo, M.; Zanin, C.; Vayssiére, J. L.; Petit, P. X.; Kroemer, G. *J. Exp. Med.* **1995**, *181*, 1661.
18. Sato, A.; Fujiwara, H.; Oku, H.; Ishiguro, K.; Ohizumi, Y. *J. Pharmacol. Sci.* **2004**, *95*, 33.
19. Wada, T.; Penninger, J. M. *Oncogene* **2004**, *23*, 2838.
20. Chen, M.; Wang, J. *Apoptosis* **2002**, *7*, 313.
21. Lassus, P.; Opitz-Araya, X.; Lazebnik, Y. *Science* **2002**, *297*, 1352.
22. Wu, X.; Cao, S.; Goh, S.; Hsu, A.; Tan, B. K. H. *Planta. Med.* **2002**, *68*, 198.